Theoretical uncertainty of quasielastic neutrino cross sections from superscaling with relativistic effective mass

Jose Enrique Amaro

Universidad de Granada

amaro@ugr.es

NuInt18 - GSSI - L'Aquila - Oct. 15-19, 2018

Contents

SuSAM* = Super Scaling Analysis with M^*

The SuSAM* collaboration:

- I. Ruiz Simo
- V.L. Martinez Consentino
- E. Ruiz Arriola
- J.E. Amaro

Department of Atomic, Molecular and Nuclear Physics
University of Granada

SuSAM* literature

- **Global Superscaling Analysis of Quasielastic Electron Scattering with Relativistic Effective Mass.** J.E. Amaro, V.L. Martinez-Consentino, E. Ruiz Arriola, I. Ruiz Simo, **Phys.Rev. C98 (2018),** 024627
- **Quasielastic charged-current neutrino scattering in the scaling model with relativistic effective mass.** I. Ruiz Simo, V.L. Martinez-Consentino, J.E. Amaro, E. Ruiz Arriola, **Phys.Rev. D97 (2018)** 116006
- **Fermi-momentum dependence of relativistic effective mass below saturation from superscaling of quasielastic electron scattering**, V.L. Martinez-Consentino, I. Ruiz Simo, J.E. Amaro, E. Ruiz Arriola. Oct 13, 2017. **Phys.Rev. C96 (2017)** 064612
- **Superscaling analysis of quasielastic electron scattering with relativistic effective mass**, J.E. Amaro, E. Ruiz Arriola, I. Ruiz Simo. **Phys.Rev. D95 (2017)** 076009
- **Scaling violation and relativistic effective mass from quasi-elastic electron scattering: Implications for neutrino reactions** J.E. Amaro, E. Ruiz Arriola, I. Ruiz Simo, **Phys.Rev. C92 (2015)** 054607

Relativistic Mean Field theory of nuclear matter

Relativistic Mean field approximation of quantum hadrodynamics (QHD).
Walecka model of nuclear matter (σ-ω exchange).
Dirac equation with strong scalar and vector potentials

$$[\boldsymbol{\alpha} \cdot \mathbf{p} + \beta(m_N - g_\sigma S)]\, u(\mathbf{p}) = (E - g_\omega V) u(\mathbf{p}) \tag{1}$$

Relativistic scalar (S) and vector (V) potentials: ground state expectation values of meson fields

$$S = \langle \sigma \rangle \qquad V = \langle \omega^0 \rangle. \tag{2}$$

Equivalent to the free Dirac equation with a effective mass

$$m_N^* = m_N - g_\sigma S \tag{3}$$

and effective energy

$$E^* = E - g_\omega V \tag{4}$$

Energy-momentum relation

$$E^* = \sqrt{\mathbf{p}^2 + m_N^{*2}} \tag{5}$$

Saturation of nuclear matter

S and M_N^* are computed with self-consistent Hartree equations

$$S = \frac{g_\sigma}{m_\sigma^2}\rho_S \qquad \rho_S = \frac{4}{(2\pi)^3}\int_0^{k_F} d^3p \frac{m_N^*}{E^*(\mathbf{p})}$$

The saturation curve for nuclear matter is obtained (binding energy per particle)

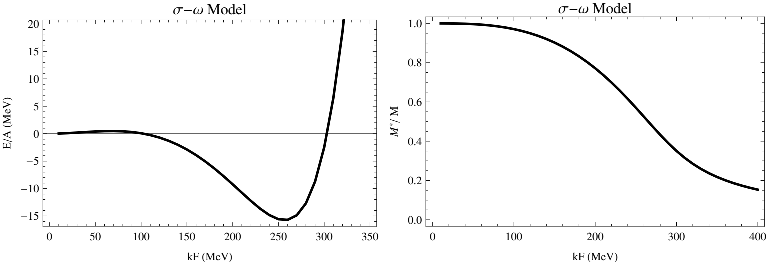

In the SuSAM* model $M^* = m_N^*/m_N$ and k_F are fitted to (e,e') data.

Quasielastic electron scattering

The quasielastic (e, e') cross section

$$\frac{d\sigma}{d\Omega' d\epsilon'} = \sigma_{\mathrm{Mott}}(v_L R_L + v_T R_T). \tag{6}$$

σ_{Mott} is the Mott cross section

$$v_L = \frac{Q^4}{q^4} \tag{7}$$

$$v_T = \tan^2 \frac{\theta}{2} - \frac{Q^2}{2q^2}. \tag{8}$$

q: momentum transfer
ω: energy transfer
θ: scattering angle
$Q^2 = \omega^2 - q^2 < 0$: the squared four-momentum transfer
$R_L(q, \omega)$, $R_T(q, \omega)$: longitudinal and transverse response functions

Nuclear responses in the RMF

RMF model of nuclear matter:

- one-particle one-hole (1p-1h) excitations in the nuclear medium
- one-body electromagnetic current operator,
- the initial and final nucleons have the same effective mass m_N^*.
- initial nucleon energy in the mean field $E = \sqrt{\mathbf{p}^2 + {m_N^*}^2}$, $p < k_F$.
- final momentum of the nucleon $\mathbf{p}' = \mathbf{p} + \mathbf{q}$,
- Pauli blocking: $p' > k_F$.
- final nucleon energy $E' = \sqrt{\mathbf{p}'^2 + {m_N^*}^2}$.

The nuclear response functions are proportional to the scaling function

$$R_K = r_K f^*(\psi^*), \qquad K = L, T \tag{9}$$

r_L and r_T: single-nucleon response functions,
$f^*(\psi^*)$: the scaling function,

Scaling function of nuclear matter in the RMF

The scaling function of nclear matter in the RMF is the same as that of the RFG

$$f^*(\psi^*) = f_{\mathrm{RFG}}(\psi^*) = \frac{3}{4}(1-\psi^{*2})\theta(1-\psi^{*2}) \tag{10}$$

But the scaling variable is DIFFERENT

It is obtained by replacing $m_N \to m_N^*$ in the RFG equations.

Introduce the dimensionless variables

$$\begin{aligned}
\lambda &= \omega/2m_N^*, & (11)\\
\kappa &= q/2m_N^*, & (12)\\
\tau &= \kappa^2-\lambda^2, & (13)\\
\eta_F &= k_F/m_N^*, & (14)\\
\xi_F &= \sqrt{1+\eta_F^2}-1, & (15)\\
\epsilon_F &= \sqrt{1+\eta_F^2}, & (16)
\end{aligned}$$

Scaling variable with relativistic effective mass

The minimum energy for the initial nucleon that is allowed to absorb the energy and momentum transfer (q, ω). (in units of m_N^*)

$$\epsilon_0 = \mathrm{Max}\left\{\kappa\sqrt{1+\frac{1}{\tau}} - \lambda, \epsilon_F - 2\lambda\right\}, \tag{17}$$

The scaling variable is defined as

$$\psi^* = \sqrt{\frac{\epsilon_0 - 1}{\epsilon_F - 1}}\mathrm{sgn}(\lambda - \tau). \tag{18}$$

ψ^* is negative to the left of the quasielastic peak (defined by $\lambda = \tau$) and positive on the right side.

Electromagnetic current operator

We use the CC2 prescription of the electromagnetic current operator

$$J^{\mu}_{s's} = \overline{u}_{s'}(\mathbf{p}') \left[F_1 \gamma^{\mu} + F_2 i \sigma^{\mu\nu} \frac{Q_{\nu}}{2m_N} \right] u_s(\mathbf{p}) \tag{19}$$

F_i are the Pauli form factors of the nucleon,
The spinors contain the effective mass instead of the bare nucleon mass
$\Longrightarrow$ enhancement of lower components
$\Longrightarrow$ The current matrix element differs from the bare nucleon
$\Longrightarrow$ enhancement of transverse current
$\Longrightarrow$ enhancement of transverse response
As a consequence the electric and magnetic form factors are modified in the medium

$$G^*_E = F_1 - \tau \frac{m^*_N}{m_N} F_2 \tag{20}$$

$$G^*_M = F_1 + \frac{m^*_N}{m_N} F_2. \tag{21}$$

Single-nucleon response functions

$$r_K = \frac{\xi_F}{m_N^* \eta_F^3 \kappa}(ZU_K^p + NU_K^n) \qquad (22)$$

for Z protons and N neutrons.
U_L, U_T are computed from the matrix elements of the electromagnetic current operator.

$$U_L = \frac{\kappa^2}{\tau}\left[(G_E^*)^2 + \frac{(G_E^*)^2 + \tau(G_M^*)^2}{1+\tau}\Delta\right] \qquad (23)$$

$$U_T = 2\tau(G_M^*)^2 + \frac{(G_E^*)^2 + \tau(G_M^*)^2}{1+\tau}\Delta \qquad (24)$$

$$\Delta = \frac{\tau}{\kappa^2}\xi_F(1-\psi^{*2})\left[\kappa\sqrt{1+\frac{1}{\tau}} + \frac{\xi_F}{3}(1-\psi^{*2})\right]. \qquad (25)$$

This is a small correction around the QE peak $-1 < \psi^* < 1$ because it is proportional to the small quantity ξ_F.

The SuSAM* approach

- **The cross section is computed by using the RMF equations**
- **But using a phenomenological scaling function fitted to experimental data.**
- The experimental scaling function $f^*_{\rm exp}$ data are computed by dividing the experimental cross section by the single nucleon contribution

$$f^*_{\rm exp} = \frac{\left(\frac{d\sigma}{d\Omega' d\epsilon'}\right)_{\rm exp}}{\sigma_{\rm Mott}\left(v_L r_L + v_T r_T\right)}$$

- We tune M^* and k_F to find the best scaling of data

SuSAM* analysis of ^{12}C

- (a) $M*$ scaling analysis of the experimental data of ^{12}C compared to the RFG parabola.
- $M^* = 0.8$ and $k_F = 225$ MeV/c
- Scaling is violated but a large fraction of the data collapse into a data cloud surrounding the RFG parabola
- (b): RFG Monte Carlo simulation of QE data with relativistic effective mass $M^* = 0.8 \pm 0.1$.

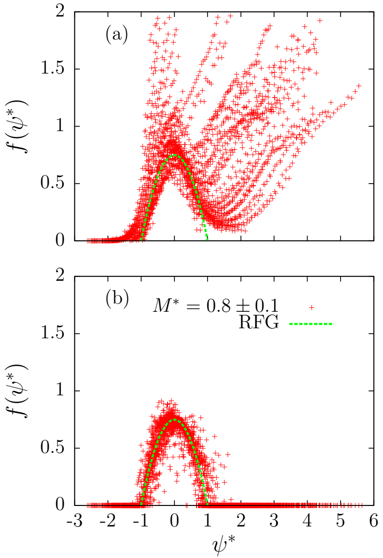

The SuSAM* phenomenological quasielastic peak

- Data selection by computing the data density
- $n =$ number of points inside a $(r = 0.1)$ circle
- All selected points with $n > m$ are considered "quasielastic" within an uncertainty band
- For the SuSAM* we choose the case $m = 25$, where a well defined data band is obtained

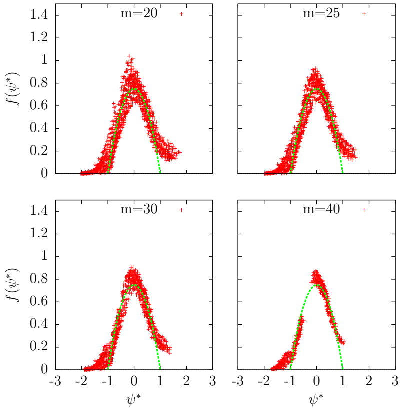

Phenomenological M^*-scaling function for ^{12}C.

$$f^*(\psi^*) = a_3 e^{-(\psi^* - a_1)^2/(2a_2^2)} + b_3 e^{-(\psi^* - b_1)^2/(2b_2^2)} \qquad \text{(Band A)}$$

- $f^*(\psi^*)$ and the uncertainty band, $f^*_{min} < f^* < f^*_{max}$, are fitted to experimental data.
- Well described as sum of two Gaussians
- Only data with density $n \geq 25$ inside a $(r = 0.1)$ circle are included.
- $\simeq 1000$ QE data / 2500 are described by the band

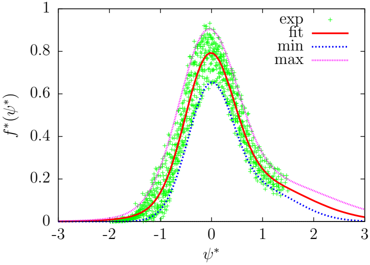

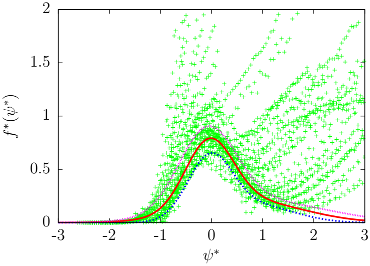

Data are from
O. Benhar, D. Day and I. Sick,
arXiv:nucl-ex/0603032.
http://faculty.virginia.edu/qes-archive/

Global fits of SuSAM* parameters

Fits to (e, e') data for nuclei: ^{2}H, ^{3}H, ^{3}He, ^{4}He, ^{12}C, ^{6}Li, ^{9}Be, ^{24}Mg, ^{59}Ni, ^{89}Y, ^{119}Sn, ^{181}Ta, ^{186}W, ^{197}Au, ^{16}O, ^{27}Al, ^{40}Ca, ^{48}Ca, ^{56}Fe, ^{208}Pb, and ^{238}U.

- Separate fits for each nucleus to the ^{12}C scaling function
- Global fit of all the data including the scaling function parameters.

- Errors ΔM^* and Δk_F are computed in a χ^2 fit.
- Results are compared to the $\sigma - \omega$ model of Serot and Walecka, Adv.Nucl.Phys.16(1986)1.

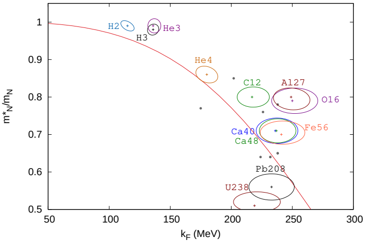

SuSAM* scaling bands

4230 QE data for ALL nuclei: ^{2}H, ^{3}H, ^{3}He, ^{4}He, ^{12}C, ^{6}Li, ^{9}Be, ^{24}Mg, ^{59}Ni, ^{89}Y, ^{119}Sn, ^{181}Ta, ^{186}W, ^{197}Au, ^{16}O, ^{27}Al, ^{40}Ca, ^{48}Ca, ^{56}Fe, ^{208}Pb, and ^{238}U.

- (e, e') data are scaled with the best parameters of the global fit and selected with the density criterion.
- band C (in pink): global fit
- band B (in green): ^{12}C band

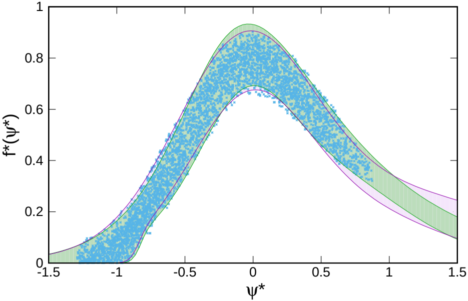

Data are from Benhar, Day and Sick http://faculty.virginia.edu/qes-archive/

Parametrization of SuSAM* bands B, C:

$$f^*(\psi^*) = \frac{a_3 e^{-(\psi^*-a_1)^2/(2a_2^2)} + b_3 e^{-(\psi^*-b_1)^2/(2b_2^2)}}{1 + e^{-\frac{\psi^*-c_1}{c_2}}}$$

Scaling of world data with SuSAM* parameters

^{2}H, ^{3}H, ^{3}He, ^{4}He, ^{12}C, ^{6}Li, ^{9}Be, ^{24}Mg, ^{59}Ni, ^{89}Y, ^{119}Sn, ^{181}Ta, ^{186}W, ^{197}Au, ^{16}O, ^{27}Al, ^{40}Ca, ^{48}Ca, ^{56}Fe, ^{208}Pb, and ^{238}U.

- (e, e') world data scaled with the best parameters of the global fit
- $\simeq$ 9000 / 20000 data inside band C
- 4230 data are true quasielastic
- Points outside of the band are non-quasielastic (delta-peak, inelastic, or low-energy regions)
- The scaling band estimates the theoretical uncertainty of the QE peak description in the SuSAM* model.

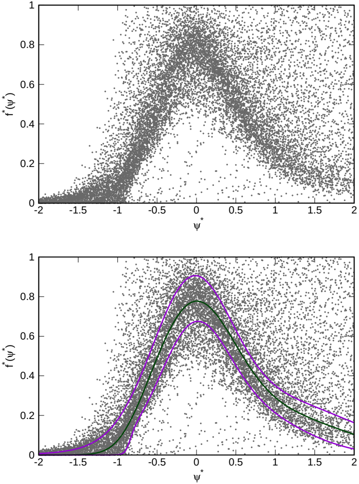

Data are from Benhar, Day and Sick http://faculty.virginia.edu/qes-archive/

SuSAM* quasielastic (e, e') predictions for ^{2}H

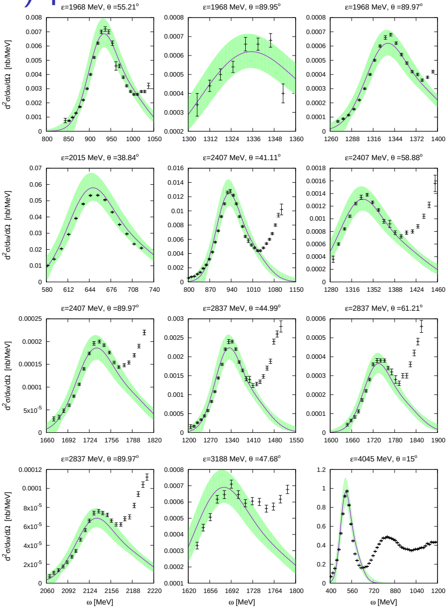

- (e, e') cross section data for ^{2}H
- Compared to the SuSAM* QE model
- band B
- $k_F = 82$ MeV/c
- $M^* = 1$

SuSAM* (e, e') predictions ^{3}H

- $k_F = 136$ MeV/c
- $M^* = 0.98$

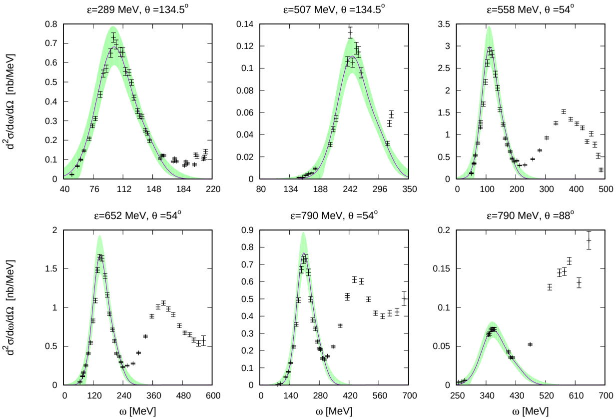

SuSAM* quasielastic (e, e') predictions for ^{3}He

- $k_F = 130$ MeV/c
- $M^* = 0.98$

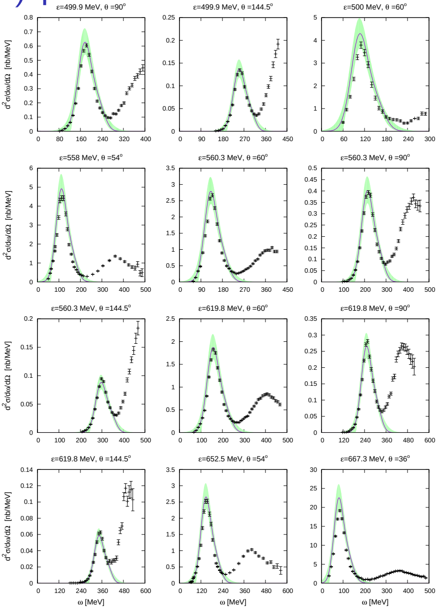

SuSAM* (e, e') predictions: ^{4}He

- $k_F = 180$ MeV/c
- $M^* = 0.86$

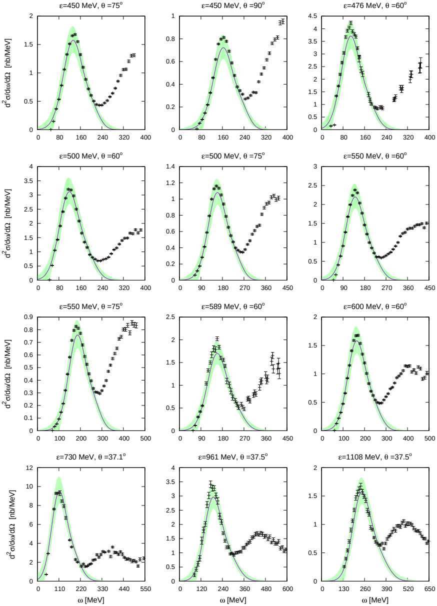

SuSAM* (e, e') predictions: ^{12}C

- $k_F = 217$ MeV/c
- $M^* = 0.8$

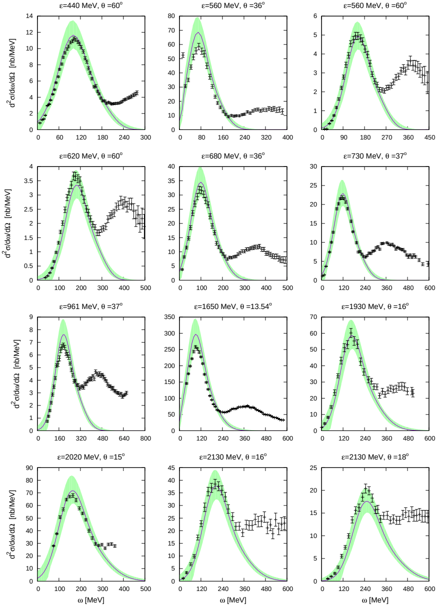

SuSAM* (e, e') predictions ^{16}O

- $k_F = 230$ MeV/c
- $M^* = 0.8$

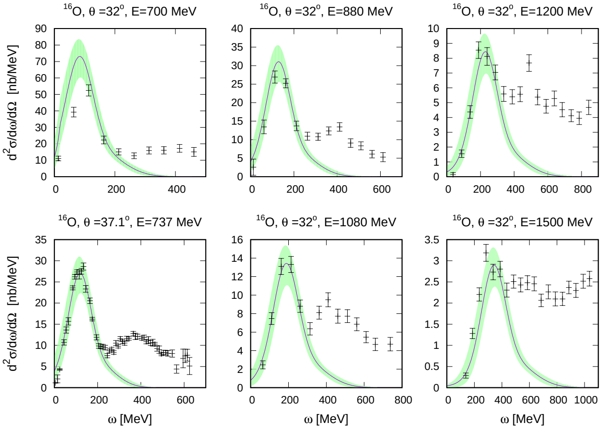

SuSAM* (e, e') predictions - Light to heavy nuclei

- $k_F = 175 — 238$ MeV/c
- $M^* = 0.77 — 0.78$

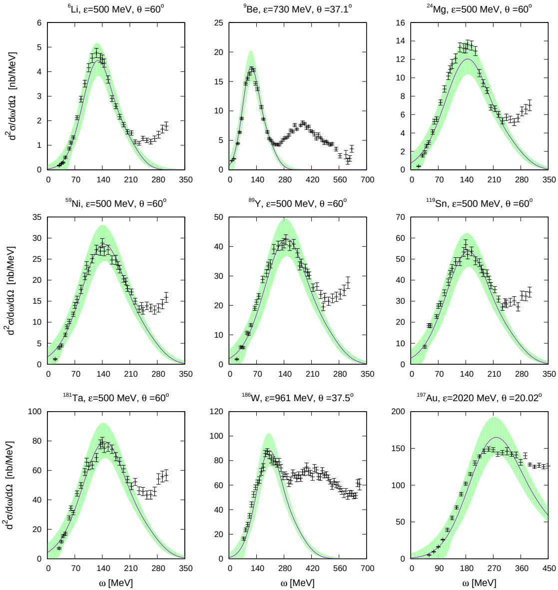

SuSAM* (e, e') predictions ^{27}Al

- $k_F = 249$ MeV/c
- $M^* = 0.8$

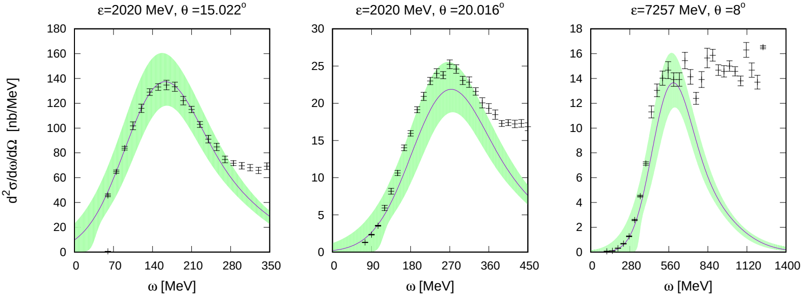

SuSAM* (e, e') predictions - ^{40}Ca

- $k_F = 236\text{MeV}/c$
- $M^* = 0.8$

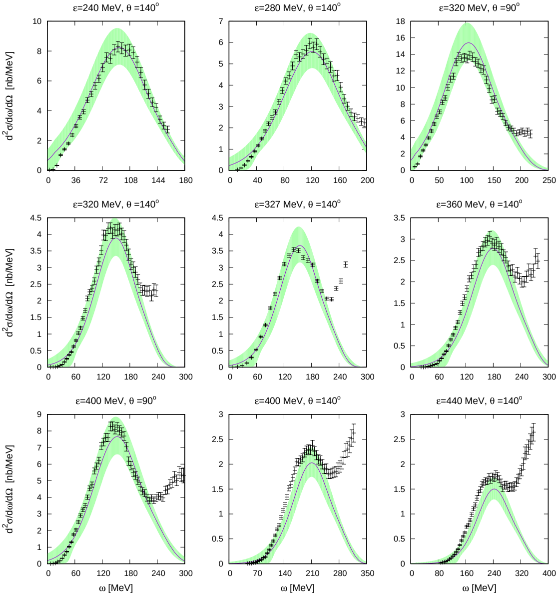

SuSAM* (e, e') predictions - ^{48}Ca

- $k_F = 236\text{MeV}/c$
- $M^* = 0.8$

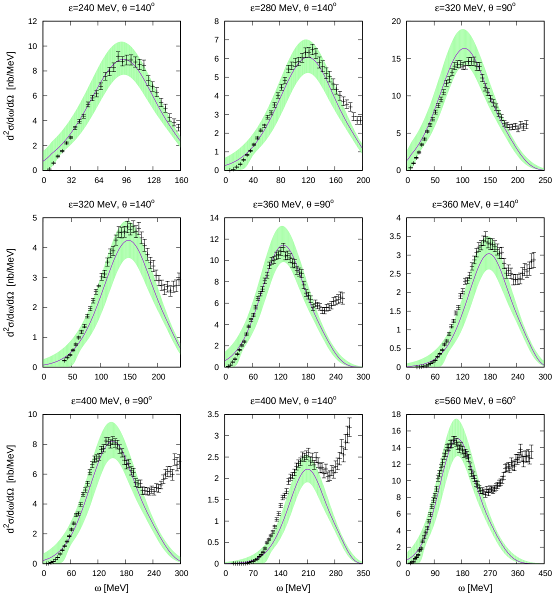

SuSAM* (e, e') predictions - ^{56}Fe

- $k_F = 240\text{MeV}/c$
- $M^* = 0.7$

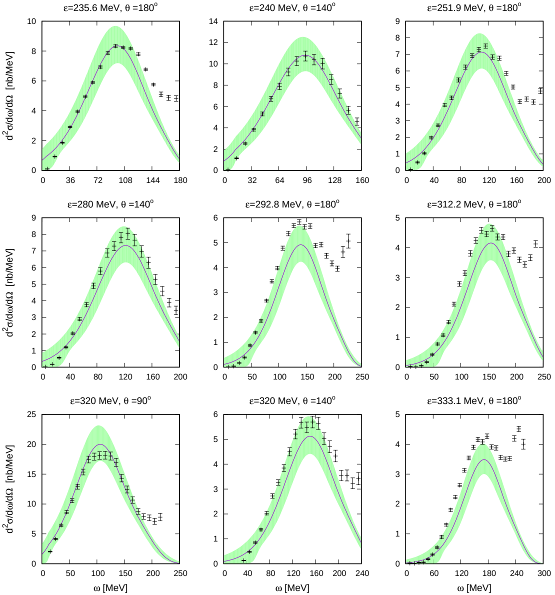

SuSAM* (e, e') predictions ^{208}Pb

- $k_F = 233$ MeV/c
- $M^* = 0.56$

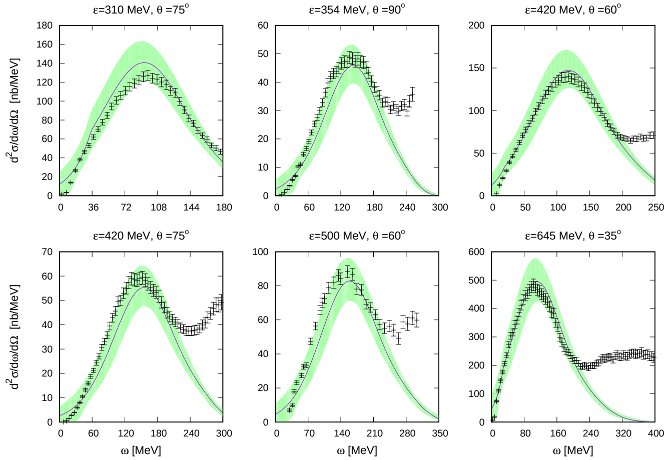

SuSAM* (e, e') predictions ^{40}Ar

- $k_F = 217$ MeV/c for $A = 12$
- $k_F = 240$ MeV/c for $A = 48, 40$

Inclusive (e, e') for ^{12}C, ^{48}Ti and ^{40}Ar
$\epsilon = 2222$ MeV, $\theta = 15.541^{\text{o}}$,

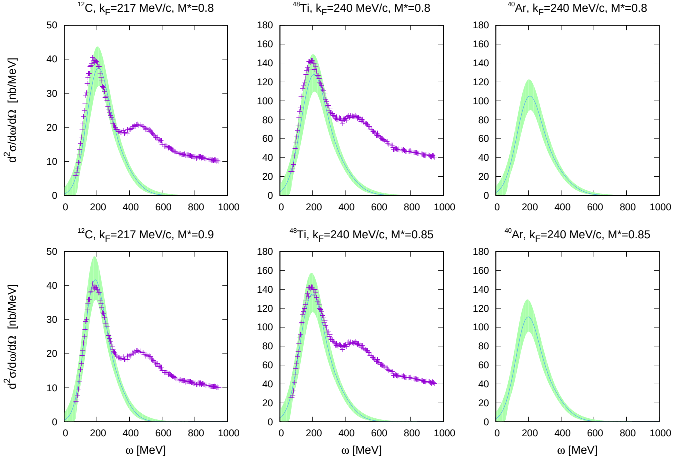

Data from the recent JLab experiment H. Dai et al., (JLab Hall A Collaboration), **Phys. Rev. C98 (2018)** 014617.

Quasielastic CC neutrino scattering

For (ν_μ, μ^-) or $(\overline{\nu}_\mu, \mu^+)$ reactions
Lepton energies: $\epsilon = E_\nu$ and $\epsilon' = m_\mu + T_\mu$,
Lepton momenta: $\mathbf{k}, \mathbf{k}'$.
four-momentum transfer $k^\mu - k'^\mu = (\omega, \mathbf{q})$, with $Q^2 = q^2 - \omega^2 > 0$.
Scattering angle: θ_μ,

Double-differential cross section

$$\frac{d^2\sigma}{dT_\mu d\cos\theta_\mu} = \sigma_0 \{ V_{CC} R_{CC} + 2V_{CL} R_{CL} + V_{LL} R_{LL} + V_T R_T \pm 2V_{T'} R_{T'} \} ,$$

Is a linear combination of five weak response functions $R_K(q, \omega)$ with leptonic coefficients V_K

$$\sigma_0 = \frac{G^2 \cos^2\theta_c}{4\pi} \frac{k'}{\epsilon} v_0 .$$

$G = 1.166 \times 10^{-11} \quad \mathrm{MeV}^{-2}$: weak Fermi constant,
Cabibbo angle: $\cos\theta_c = 0.975$,
kinematic factor $v_0 = (\epsilon + \epsilon')^2 - q^2$.

Leptonic factors and response functions

V_K coefficients: depend only on the lepton kinematics

$$
\begin{aligned}
V_{CC} &= 1-\delta^2\frac{Q^2}{v_0} \\
V_{CL} &= \frac{\omega}{q}+\frac{\delta^2}{\rho'}\frac{Q^2}{v_0} \\
V_{LL} &= \frac{\omega^2}{q^2}+\left(1+\frac{2\omega}{q\rho'}+\rho\delta^2\right)\delta^2\frac{Q^2}{v_0} \\
V_T &= \frac{Q^2}{v_0}+\frac{\rho}{2}-\frac{\delta^2}{\rho'}\left(\frac{\omega}{q}+\frac{1}{2}\rho\rho'\delta^2\right)\frac{Q^2}{v_0} \\
V_{T'} &= \frac{1}{\rho'}\left(1-\frac{\omega\rho'}{q}\delta^2\right)\frac{Q^2}{v_0}.
\end{aligned}
$$

where $\delta = m_\mu/\sqrt{Q^2}$
$\rho = Q^2/q^2$,
$\rho' = q/(\epsilon+\epsilon')$.

Nuclear response functions are the components of the hadronic tensor:

$$R_{CC} = W^{00} \quad (26)$$

$$R_{CL} = -\frac{1}{2}(W^{03}+W^{30}) \quad (27)$$

$$R_{LL} = W^{33} \quad (28)$$

$$R_T = W^{11}+W^{22} \quad (29)$$

$$R_{T'} = -\frac{i}{2}(W^{12}-W^{21}). \quad (30)$$

Weak responses in the SuSAM* model

1p-1h excitations of nucleons in the RMF with effective mass m_N^*.
Nuclear response function R_K:

$$R_K = r_K f^*(\psi^*)$$

is proportional to a single-nucleon response function r_K times the scaling function $f^*(\psi^*)$
SuSAM* : use the phenomenological scaling band extracted from (e, e').

$$r_K = \frac{\xi_F^*}{m_N^* \eta_F^{*3} \kappa^*} \mathcal{N} U_K$$

where $\mathcal{N} = N, Z$.
The single nucleon reduced responses U_K are analytical.

CC current matrix elements

Single nucleon CC current: $J^\mu = V^\mu - A^\mu$
Vector current:

$$V^\mu_{s's} = \overline{u}_{s'}(\mathbf{p}') \left[2F_1^V \gamma^\mu + 2F_2^V i\sigma^{\mu\nu} \frac{Q_\nu}{2m_N} \right] u_s(\mathbf{p}) \qquad (31)$$

$F_i^V = (F_i^P - F_i^N)/2$ the isovector form factors of the nucleon.
Axial current:

$$A^\mu_{s's} = \overline{u}_{s'}(\mathbf{p}') \left[G_A \gamma^\mu \gamma_5 + G_P \frac{Q^\mu}{2m_N} \gamma_5 \right] u_s(\mathbf{p}) \qquad (32)$$

The relativistic effective mass in the initial and final spinors $u_s(\mathbf{p})$, and $u_{s'}(\mathbf{p}')$, modifies the values of the matrix elements in the medium

SuSAM* predictions for CCQE neutrino scattering

Flux-averaged double differential cross section

$$\frac{d^2\sigma}{dT_\mu d\cos\theta_\mu} = \frac{1}{\Phi_{tot}} \int dE_\nu \Phi(E_\nu) \frac{d^2\sigma}{dT_\mu d\cos\theta_\mu}(E_\nu)\,, \qquad (33)$$

$\frac{d^2\sigma}{dT_\mu d\cos\theta_\mu}(E_\nu)$: the SuSAM* cross section

neutrino energy E_ν.

Neutrino flux: $\Phi(E_\nu)$

SuSAM* predictions for MiniBooNE, (ν_μ, μ^-)

Each panel is labeled by the mean value of $\cos\theta_\mu$ in the experimental bin.

Experimental data are from MiniBooNE

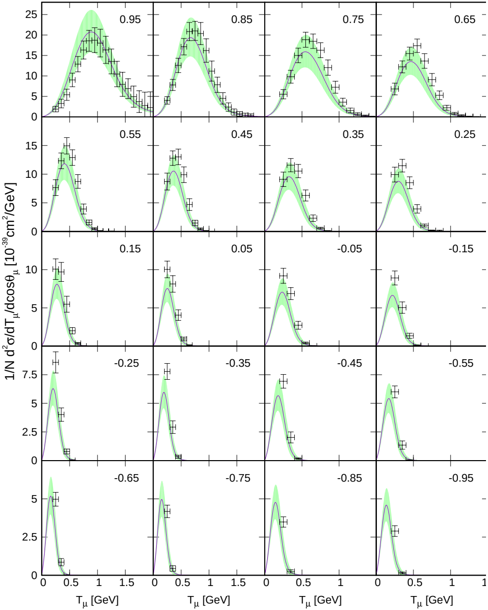

SuSAM* predictions for MiniBooNE, $(\bar{\nu}_\mu, \mu^+)$

Each panel is labeled by the mean value of $\cos\theta_\mu$ in the experimental bin.

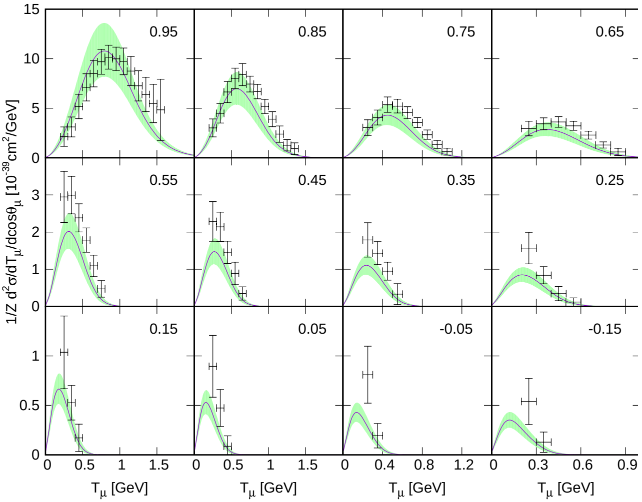

SuSAM* predictions for MiniBooNE

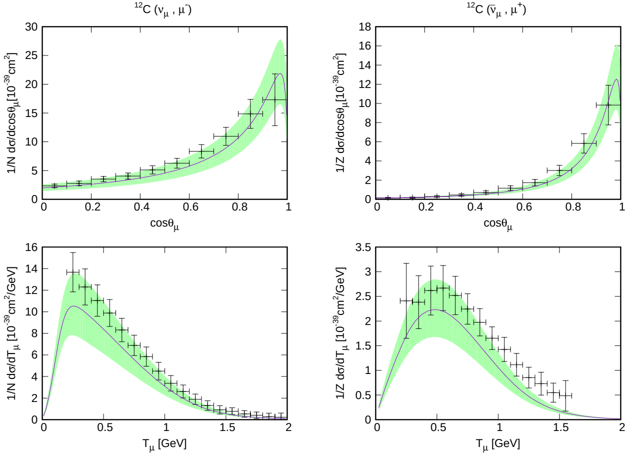

Flux-integrated single-differential cross sections per target neutron (proton) for the CCQE neutrino (antineutrino) reactions on ^{12}C in the SuSAM* model.
Left panels are for neutrinos and right ones for antineutrinos.
The experimental data are from MiniBooNE

SuSAM* predictions for T2K ^{12}C (ν_μ, μ^-)

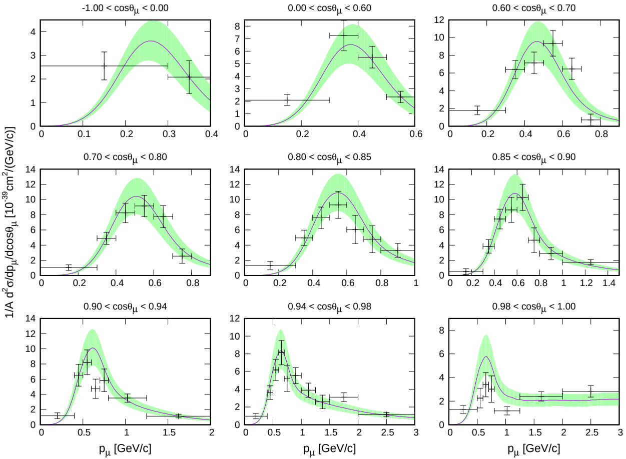

T2K flux-folded double differential CCQE cross section per nucleon for ν_μ scattering on ^{12}C in the SuSAM* model.
Experimental data are from T2K

SuSAM* predictions for T2K ^{16}O (ν_μ, μ^-)

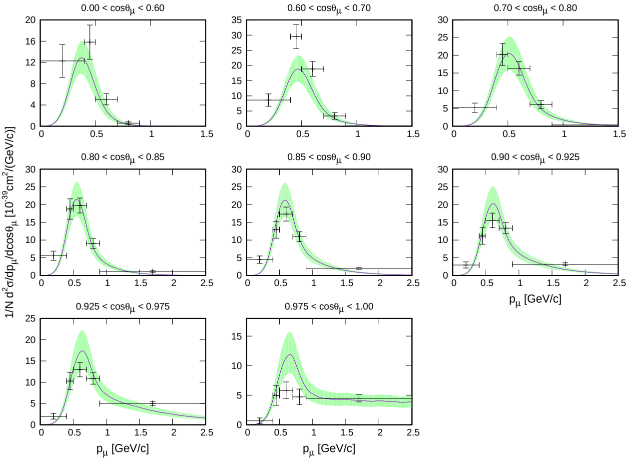

T2K flux-folded double differential CCQE cross section per nucleon for ν_μ scattering on ^{16}O in the SuSAM* model.
Experimental data are from T2K

SuSAM* predictions for T2K ^{12}C (ν_μ, μ^-)

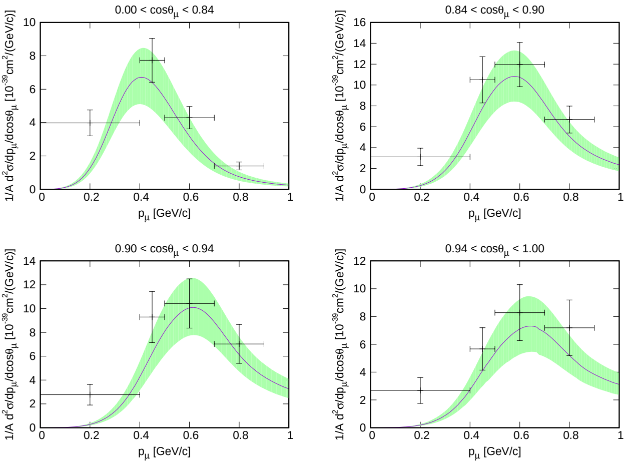

T2K flux-folded double differential CC inclusive cross section per nucleon for ν_μ scattering on ^{12}C in the SuSAM* model.
Experimental data are from T2K

SuSAM* predictions for T2K ^{12}C (ν_e, e^-)

T2K flux-folded single differential CC inclusive cross section per nucleon for ν_e scattering

The neutron binding energy in Q^2_{QE} is $E_B = 25$ MeV.

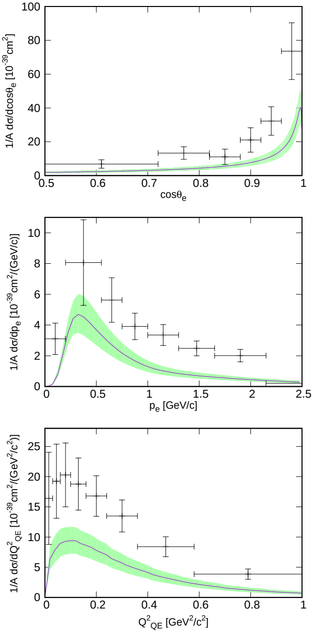

SuSAM* predictions for MINERvA Q^2_{QE} distributions

Flux-folded CCQE
(ν_μ, μ^-) from ^{12}C
$(\bar{\nu}_\mu, \mu^+)$ from CH

The data are from MINERvA

The H contribution is obtained from the elastic antineutrino-proton cross section divided by $Z = 7$.

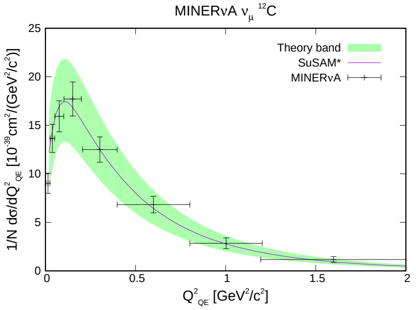

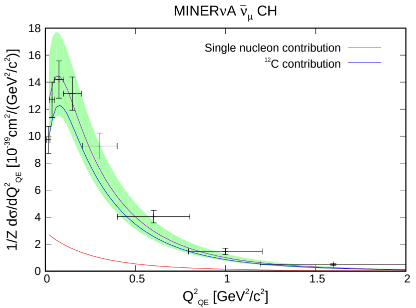

SuSAM* predictions for MINERvA CCQE $(\overline{\nu}_\mu, \mu^+)$

Flux-folded double-differential cross section $\frac{d^2\sigma}{dp_{||}\, dp_\perp}$

- Antineutrino CCQE scattering from CH
- Compared to the MINERvA experiment.
- The $\overline{\nu}_\mu - H$ cross section is divided by $A = 13$.
- $\theta_\mu < 20^o$ cut

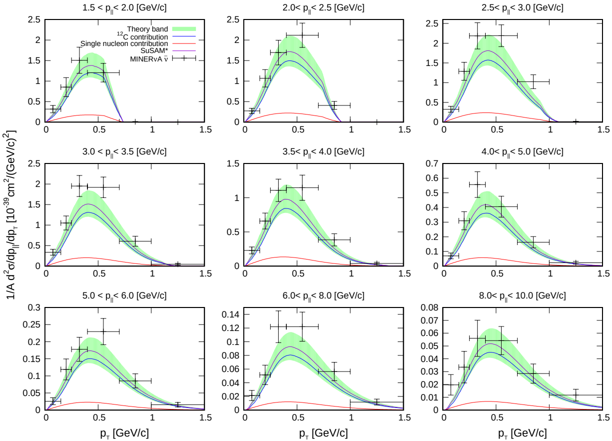

CONCLUSIONS

- SuSAM* is a **new scaling approach based on the RMF** theory of nuclear matter. It depends on M^* and k_F
- The **phenomenological scaling function** is extracted from a selection of (e, e') QE data that approximately **scale into a band**.
- The SuSAM* band has been parametrized and it provides a **global description of the QE** (e, e') **cross section** for all the nuclei considered.
- The width of the SuSAM* band represents the theoretical uncertainty of the model from effects breaking the factorization of the cross section (such as **MEC, FSI, Long and short-range correlations**)
- **SuSAM* can be applied to predict inclusive neutrino cross secions and the theoretical error.**
- In future work we will reduce the SuSAM* errors by including additional nuclear effects such as 2p-2h MEC